

Kinematic model of a translational slide in the Cidu section of the Formosan Freeway

Chia-Ming Lo, Hung-Hui Li & Chien-Chung Ke

Landslides

Journal of the International Consortium
on Landslides

ISSN 1612-510X

Landslides

DOI 10.1007/s10346-015-0650-x



Your article is protected by copyright and all rights are held exclusively by Springer-Verlag Berlin Heidelberg. This e-offprint is for personal use only and shall not be self-archived in electronic repositories. If you wish to self-archive your article, please use the accepted manuscript version for posting on your own website. You may further deposit the accepted manuscript version in any repository, provided it is only made publicly available 12 months after official publication or later and provided acknowledgement is given to the original source of publication and a link is inserted to the published article on Springer's website. The link must be accompanied by the following text: "The final publication is available at link.springer.com".

Landslides

DOI 10.1007/s10346-015-0650-x

Received: 26 June 2015

Accepted: 7 October 2015

© Springer-Verlag Berlin Heidelberg 2015

Chia-Ming Lo · Hung-Hui Li · Chien-Chung Ke

Kinematic model of a translational slide in the Cidu section of the Formosan Freeway

Abstract This study presents a kinematic model of a translational slide in the Cidu section of the Formosan Freeway in Taiwan, including the associated kinematic processes and the geometry of the deposition. A numerical simulation of the slide was performed using the discrete element method. This kinematic model has been considered the distribution of bedding plane and joints, engineering installations, and mechanical parameters in the development of a numerical model capable of clarifying the kinematic characteristics of this translational slide with high velocities. When the friction coefficient of each particle was set to 0.03, the predicted maximum velocity was 23.6 m/s and the debris reached the other side of the Formosan Freeway. The simulations demonstrated that the three cars involved in the incident and the Formosan Freeway itself were buried at 2 to 4 s during the event (the predicted average velocity was 10.2 m/s) and that the translational slide ceased its movement at 7.5 s, resulting in the formation of a slightly fragmented depositional mass.

Keywords Kinematic model · Translational slide · Numerical simulation · Discrete element method

Introduction

Numerous calamities throughout the metropolitan and mountainous areas of Taiwan have been caused by translational slides. Dip slopes, at which translational slides are more likely to occur, are natural slopes (particularly of rock) in which the dip of the strata and the primary planes of weakness of the strata have the same direction with a difference in angle of less than 15°. The sudden onset and velocity of translational slides (reaching 100 km/h or 28 m/s) can lead to severe disasters (Hung 2010).

At approximately 14:29 on April 25, 2010, a dip slope slide occurred at kilometer 3.1 in the Cidu section of the Formosan Freeway, an area referred to as Shi-gong-ge-shan. A substantial amount of debris (>200,000 m³) completely buried a section of the freeway, 190 m long and 35 to 43 m wide, as well as three vehicles passing through the area. The landslide occurred on a sunny day with no recorded earth tremors, thus excluding the possibility that rainfall or an earthquake triggered the event (Wang et al. 2013). A topographical/geographical investigation conducted by Lin et al. (2010) following the disaster revealed that, prior to the event, the slope in the area was distinctly wedge-shaped with the tip protruding toward the northwest. Near Shi-gong-ge-shan, the dip slope presented a flatiron feature in four underlying layers, as shown in Fig. 1, where A marks the topmost rock section, the gentle terrain of which may have formed after the dip slope slide. The Cidu landslide occurred in the bottommost rock section, marked by D in Fig. 1. Chen et al. (2010) identified this section as a sandstone section (SS) at the bottom of the Miocene Shihti Formation (St), the thickness of which is approximately 15 to 20 m. The underlying stratum exposed by the landslide belongs to the Miocene Taliao Formation (Tl), which consists lithologically of a thick layer of shale

with occasional beds of thin sandstone formations. The contact between the two strata was identified as the primary sliding plane in the Cidu event (Fig. 2). It should be noted that the strike of rock formations in this area is NE and that the dip slopes dip toward the SE an angle of 10–30°. These rock slope characteristics in conjunction with the fact that Freeway No. 3 cuts through the dip slope increased the likelihood of a dip slope failure (Wang et al. 2013).

Following the incident, government agencies and researchers investigated the mechanisms associated with the dip slope slide and augmented efforts to monitor the stability of dip slopes near national freeways, and established an early warning system. However, there remains considerable room for improvement, particularly with regard to determining the velocity of sliding masses and their sphere of influence. Extremely high velocity landslides, particularly rockslides that develop into debris avalanches, are remarkable geological phenomena (Steven and Simon 2006). Velocity is the most important parameter determining the destructive potential of landslides (Hung 2007), and terrain-related characteristics, such as mass separation, collisional interaction, and kinematic change from slope mass sliding to particle flow, are important for estimating the sphere of influence in order to protect properties in the downstream area (Lo et al. 2011, 2014). Consequently, this study employed a discrete element program (PFC3D 3.0) to construct a numerical model of a translational slide in the Cidu section of the Formosan Freeway. Our goal was to compare the simulated deposits with those observed onsite, with the ultimate goal of clarifying the kinematic processes occurring in each stage of the landslide. The study also conducted numerical simulations of the collapse in order to estimate the speed of the landslide, which enabled us to explain the processes and characteristics of this translational slide.

Methodology

Principle of PFC3D

Particle Flow Code in 3D (PFC3D) is a program developed by Itasca in 1999 based on the discrete element method (Itasca 2002). The PFC3D model is used mainly to simulate the movement and interactions of rigid spheres (ball elements). More complex behavior can be modeled by allowing the particles to be bonded together at their contact points, such that when the inter-particle forces acting at any bond exceed the bond strength, that bond is broken. In addition, the PFC3D model also includes wall elements. The balls and walls interact with one another via the forces that arise at contacts. In addition, contacts may not form between two walls; thus, contacts are either ball-to-ball or ball-to-wall (Itasca 2002). The PFC3D model is based on the explicit finite difference method of calculating changes in the system at each time step, when the positions, amount of overlap, and relative movements of the particles are

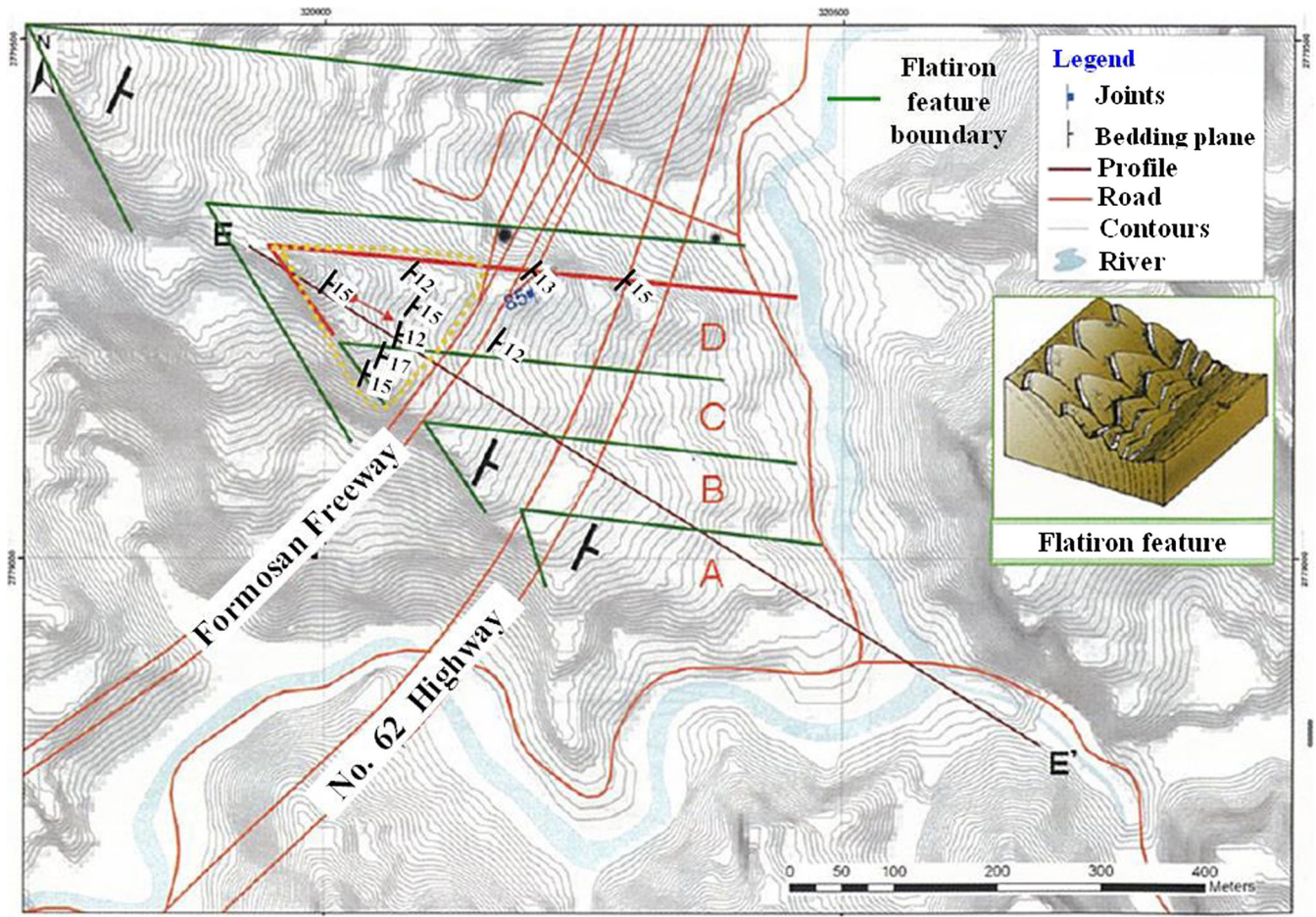


Fig. 1 Result of the geomorphologic interpretation of the slope before the disaster (Lin et al. 2010)

calculated prior to calculation of the contact force using the force–displacement law. This makes it possible to derive new velocities and positions of the particles in accordance with Newton's second law of motion.

PFC is used to calculate contact stiffness under the assumption that the stiffness of the contact between two adjacent objects is treated as normal and shear springs in series. Normal stiffness (kn) and shear stiffness (ks) are defined as follows:

$$k = \frac{k^{[A]}k^{[B]}}{k^{[A]} + k^{[B]}} \quad (1)$$

where [A] and [B] represent the two objects in contact, and k denotes normal stiffness (kn) or shear stiffness (ks).

In the slip model, given settings are used for the coefficient of friction. In the event that the slipping force at the interface between an element in contact exceeds the frictional resistance, slippage will occur, i.e., slippage occurs when the shear contact force exceeds the friction and when the contact force is equal to the friction. The bonding model includes parallel bonds between particle elements, which combine element groups into other shapes. The bond will be broken when the external force applied to the elements exceeds the bonding forces.

Numerical modeling and a comparison of deposit formations

Material parameters of the numerical model

This study used PFC3D to construct a numerical model of the dip slope slide in the Cidu section of the Formosan Freeway. The advantage of this model is its ability to simulate the bonding and separation of objects and also the substantial movements that occur after failure along weak planes and in response to the interaction effects of collision. This study referred to the setting of material parameters outlined by Potyondy and Cundall (2004). We used the results of mechanical experiments in conjunction with those obtained from PFC to conduct a preliminary conversion of macro- and micro-parameters before comparing the actual uniaxial experiments with those of simulations (Fig. 3). Thus, we could calibrate the conversion formula for the macro- and micro-parameters and derive the micro-parameters of the simulated materials.

To facilitate the simulation of energy dissipation in material collisions, we referred to the rebound coefficient obtained by Giani et al. (2004) in onsite tests (Table 1). This provided us with damping parameter settings consistent with those found in the field. The coefficient of kinetic friction is the key factor in the movement processes of dip slope landslides; however, obtaining such measurements can be difficult. Thus, this study compared the deposit formations that resulted from simulations using a variety

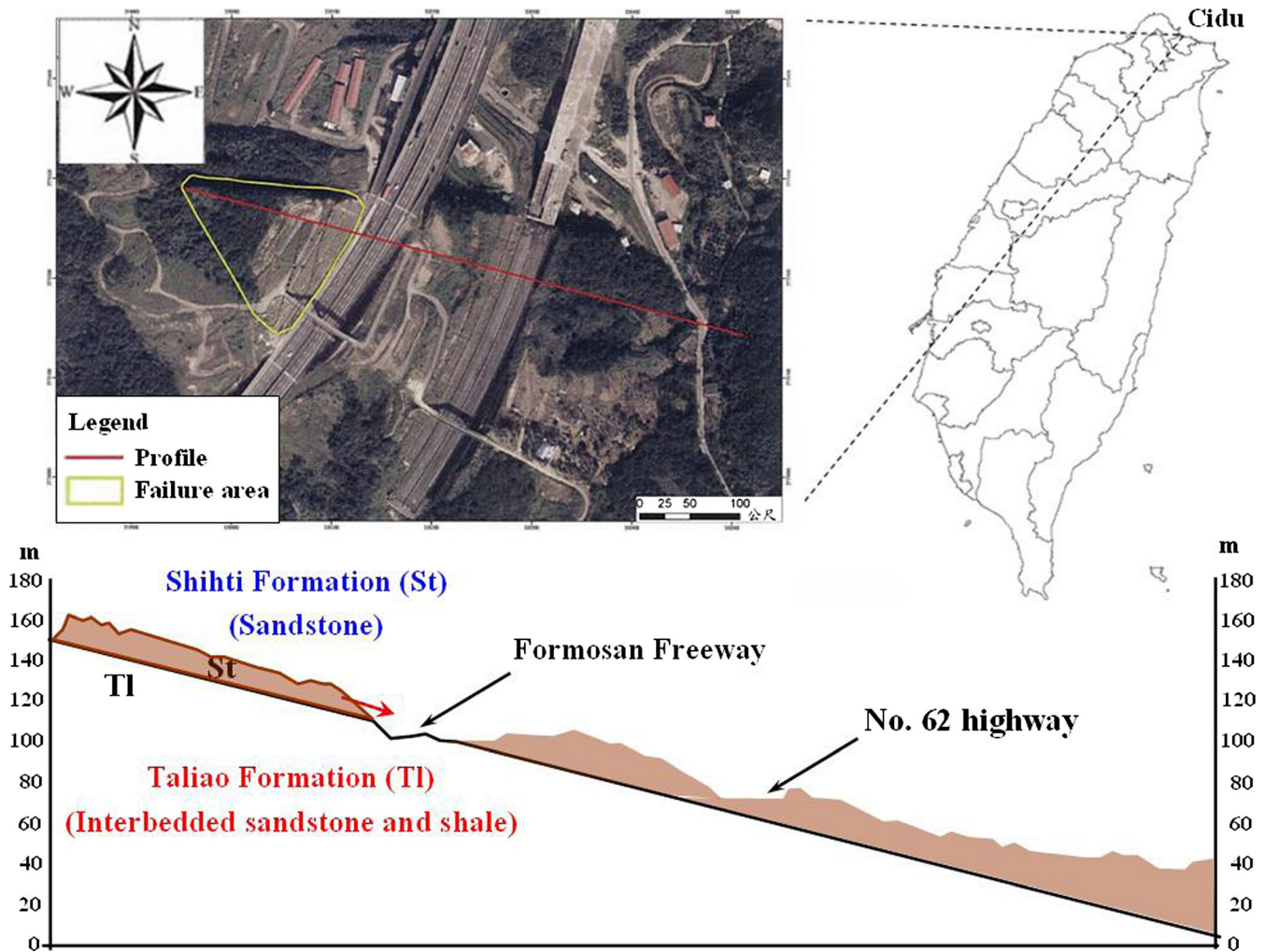


Fig. 2 Aerial photograph and geological cross section at kilometer 3.1 in the Cidu section of the Formosan Freeway (modified from Chen et al. 2010)

of coefficient settings and selected the setting that produced the result closest to the actual landslide deposit.

Full-scale numerical model

1. 3D terrain: The study adopted a post-event (2010) 1 m×1 m digital elevation model (DEM) for the source area and a pre-event (2009) 5 m×5 m DEM for the deposit area. A total of 25,342 wall elements were used for the construction of terrain, and the total length and width of the numerical model were set at approximately 842 and 376 m, respectively.
2. Sliding mass: The sliding mass included 8552 ball elements with a radius of 1.5 m. In the source area, pre-landslide terrain was constructed using wall elements with ball elements to fill the sliding mass. Once the ball elements were stable, bonding strength was applied where the ball elements came into contact with one another to form consolidated rock masses. Joints were added to the rock mass, the contact surfaces of which possessed friction settings.
3. Ground anchors: According to a summary report by the Taiwan Geotechnical Society (2011), the total number of ground anchors was 572, and each ground anchor had a strength of 60 t and a setting of 20° (angle with respect to a horizontal plane) into the dip slope. Therefore, this study used ball elements with parallel bonds (setting a 60-t tensile strength and an insertion into the dip slope of 20° for each ground anchor) to simulate the ground anchors and retaining wall at the toe of the dip slope (Fig. 4). Additionally, we fixed the bottom layer of the particles so that the upper sliding mass could slide along the top of the bottom layer of the particles. Then, the parallel bonds will play the role of the ground anchors.
4. Contact stiffness and bonding strength: Specimens obtained by on-site drilling (diameter of 10 cm and height of 25 cm) were used to perform uniaxial compression tests to determine the uniaxial compressive strength and elastic modulus. Comparisons between actual and simulated compression tests were used to revise the conversion formula in order to derive the micro-parameters of the rock in the numerical simulation (Table 2).
5. Damping coefficient: The method proposed by Giani (1992) for the conversion of viscous damping parameters was used in an experiment to obtain preliminary settings for the onsite restitution coefficient of rock collisions in the numerical simulation. The goal was to enhance consistency with the movement observed in the actual landslide.

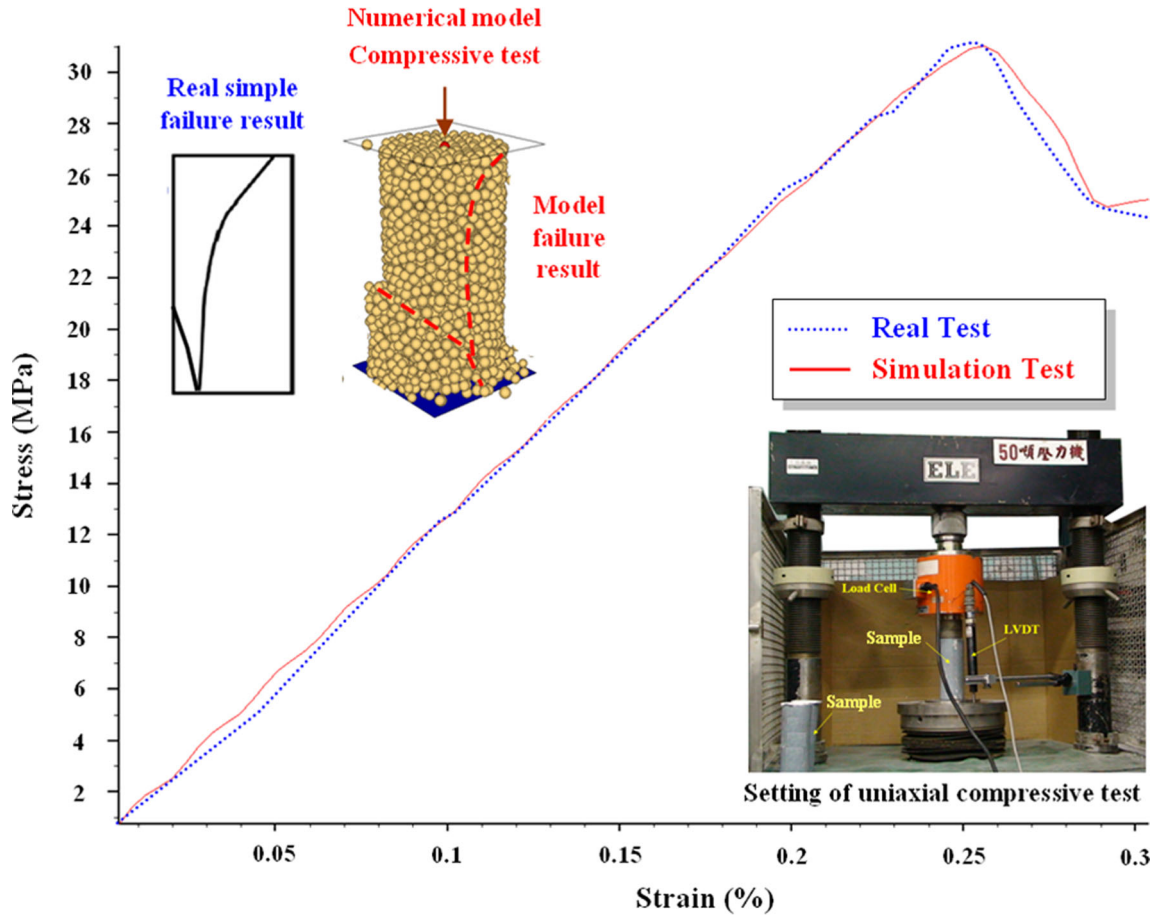


Fig. 3 Comparison of test results from simulated uniaxial compression with actual test results

- Friction coefficient: The results of a direct shear test by the Taiwan Geotechnical Society (a drilling and experiment report cited the residual shear strength of the wet shale as approximately $14\text{--}17^\circ$) were used to derive the initial settings of the friction coefficients. In the numerical simulation, the deposit formations resulting from different friction coefficient settings were compared to enable selection of the most suitable simulation parameters.
- Joint setting: Field survey results from 22 representative measurement points related to joint attitudes following the landslide (Fig. 5) revealed five sets of weak planes of weakness (including the bedding plane and joints) distributed

throughout the collapse area: joint A-1, joint A-2, joint B, joint C, and joint D. Joint A-1 exhibited a dip slope bedding plane at an attitude of $N45^\circ E/15^\circ E$ (15 measurement points). The attitudes of the four other joint sets were $N44^\circ E/45^\circ E$ (three measurement points), $N67^\circ E/60^\circ E$ (two measurement points), $N55^\circ W/55^\circ N$ (two measurement points), and $N26^\circ W/50^\circ S$ (three measurement points). The distribution of the planes of weakness has a significant influence on dip slope sliding, crumbling of the sliding mass, and the distribution of the deposit. We therefore included this information in the numerical model to increase the consistency of the simulation results.

Table 1 Conversion of on-site damping parameters (modified from Giani et al. 2004)

| | Normal restitution coefficient | Converted normal damping ratio | Shear restitution coefficient | Converted shear damping ratio |
|---|--------------------------------|--------------------------------|-------------------------------|-------------------------------|
| Bedrock slope | 0.50 | 0.21 | 0.95 | 0.02 |
| Bedrock slope covered with broken rock | 0.35 | 0.32 | 0.85 | 0.05 |
| Slope covered with rock debris and soil | 0.30 | 0.36 | 0.70 | 0.11 |
| Soil slope covered with lush vegetation | 0.25 | 0.40 | 0.55 | 0.20 |

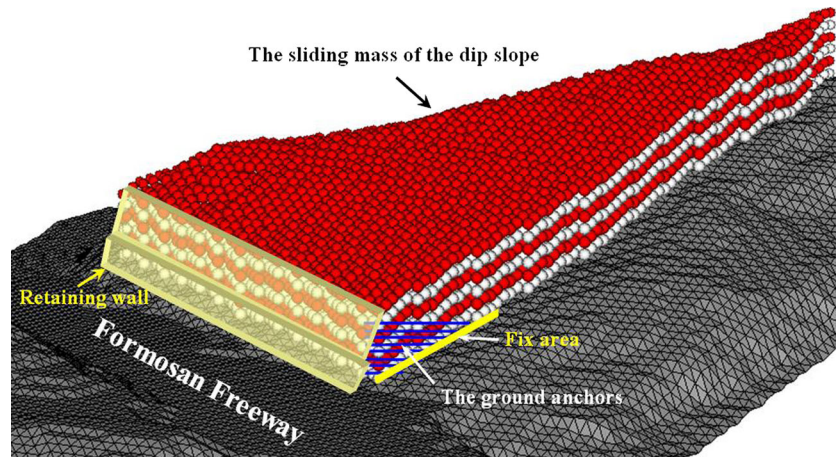


Fig. 4 Numerical model of a translational slide in the Cidu section of the Formosan Freeway

Results

Parametrical analysis

Table 3 lists the parameter combinations used in this study as well as the influence of simulation parameters on runout distance and run-up height. As shown in Tables 3 and 4, by changing the friction coefficient from 0.01 to 0.3, the runout distance was decreased and the run-up height was increased. With the lower friction coefficient of 0.01, a portion of the deposit moved south along the Formosan Freeway and another portion extended as far as highway No.62. These results are inconsistent with the actual case, which suggests that a more reasonable friction coefficient would be in the range from 0.01 to 0.3. As shown in Fig. 6 and Table 3, an increase in joint strength reduced the spread of deposited material from north to south and preserved the geometric appearance of the deposit. As shown in Table 3, higher contact stiffness expanded the spread of

the deposit, indicating that a reasonable value would be approximately 1e10 N/m.

Comparison of full-scale numerical simulation results

This study applied various friction coefficients during the simulation process (Fig. 7) to identify deposit formations most consistent with the actual deposits. The factors that we compared included run-out distance, deposition length, and deposition width. Our results revealed that a friction coefficient of 0.03 resulted in a deposited terrain that was most consistent with the formations observed in aerial photos and photogrammetry results (Table 4 and Fig. 8). Under these conditions, the maximum sliding velocity was 23.6 m/s, which enabled the entire sliding mass to reach the slope on the other side of the freeway. We therefore employed this parameter value to explain the kinematics of the dip slope slide in the Cidu section of the Formosan Freeway.

Table 2 The numerical parameters of the PFC modeling

| Parameters | Full-scale numerical model | |
|--|----------------------------|----------|
| | Rock mass | Joints |
| Number of particles | 8552 | – |
| Unit weight of ball elements (kg/m ³) | 2600 | – |
| Particle radius (m) | 1.5 | – |
| Normal stiffness (N/m) | 1.44e11 | – |
| Shear stiffness (N/m) | 7.2e10 | – |
| Friction coefficient of ball elements | 0.01–0.3 | 0.01–0.3 |
| Friction coefficient of wall elements | 0.6 | – |
| Normal stiffness of parallel bond (N/m) | 2.0e9 | – |
| Shear stiffness of parallel bond (N/m) | 1.0e9 | – |
| Normal bond strength of parallel bond (MPa) | 26 | 0.3 |
| Shear bond strength of parallel bond (MPa) | 13 | 0.1 |
| Normal damping coefficient (rock mass) | 0.36 | – |
| Shear damping coefficient (rock mass) | 0.11 | – |
| Material damping coefficient (the soil slope on the far side of the freeway) | 0.40 | – |

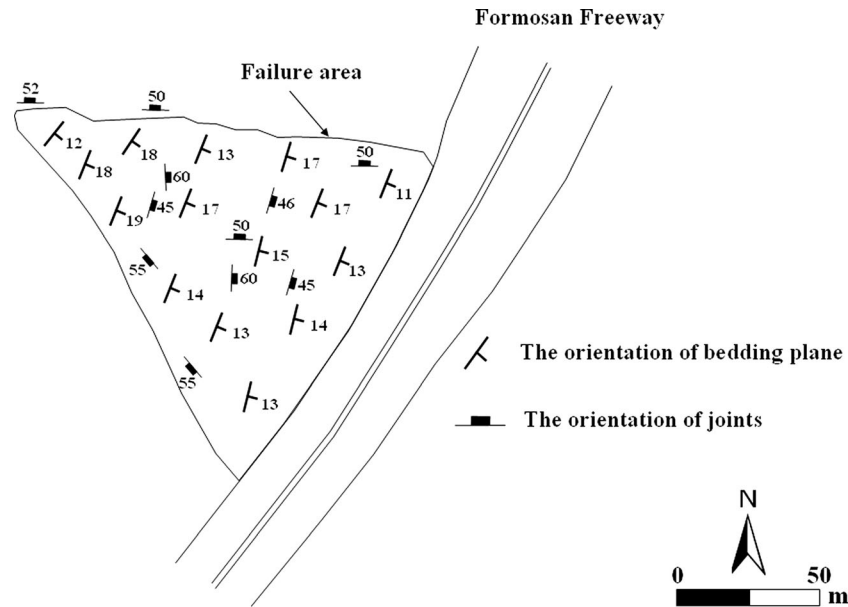


Fig. 5 Orientation of bedding plane and joints at the Cidu section of the Formosan Freeway

Kinematic processes of the Cidu translational slide

In this study, the numerical simulation was divided into two main parts. In the first part, we considered that the ground anchors were located along the toe of the dip slope, then gradually reduced the ground anchors' strength, and simulated the failure process. In the second part, almost all of the ground anchors were considered to experience failure, causing translational sliding, and the dip slope movement process was simulated. Figure 9 presents the simulation results of the first part with a friction coefficient of 0.03. The simulation results of this first part are summarized in the following points:

1. Original strength of the ground anchors (60 t): The construction of the anchor system was completed at the toe of the dip slope in 1998 (Taiwan Geotechnical Society 2011). In this kinematic model, due to the usage of the original strength of the ground anchor supports (all of ground anchors were not at failure during this stage), the dip slope did not incur displacement or deformation and the overall dip slope presented a stable state. With long-time corrosion of the anchor head, the force of each ground anchor will be reduced gradually, even to the point of failure. When we reduced the strength of the ground anchors by 0–15 %, the dip slope still not incur any displacement or deformation and the overall dip slope presented a stable state.
2. Reduction of ground anchor strength by 30 % (42 t): When the ground anchor strength was reduced by 30 %, the

displacement of the dip slope extended to 0.5–1.7 m (some tension cracks were even found on the dip slope) and caused about 6 % of the ground anchors to fail (Fig. 9a).

3. Reduction of ground anchor strength by 50 % (30 t): When the ground anchor strength was reduced by 50 %, there was about 89 % failure of ground anchors, causing the dip slope to lose support and a translational slide to begin (Fig. 9b). Field investigations by the Taiwan Geotechnical Society performed after the translational slide (April 2010) showed that only 58 anchors remained in place and that 48 % of the remaining anchors showed a fracture of their steel strands (Taiwan Geotechnical Society 2011). These field investigation results are similar to the results of the first part of the simulation. Therefore, the study used this model to perform the next step of simulation (translational slide process).

Figure 10 presents the simulation results of the second part (assume that almost all of the ground anchors have been destroyed). The landslide kinematics were divided into the following time periods:

1. 0.0–0.5 s: Almost instantaneously, the toe portion of the right wing of the sliding mass (in the direction toward Taipei, near the side of the overpass) reached a velocity of 8.2 m/s, such that the mean velocity of the entire sliding mass was 2.9 m/s (Fig. 10a).

Table 3 Tendency of runout distance and run-up height with increasing value of the different parameters

| Input parameters | Value | Runout distance | Run-up height |
|-------------------------|----------|-----------------|---------------|
| Friction coefficient | 0.01→0.3 | Decreasing | Increasing |
| Joint strength (MPa) | 0.01→100 | Decreasing | Increasing |
| Contact stiffness (N/m) | 1e8→1e11 | Increasing | Decreasing |

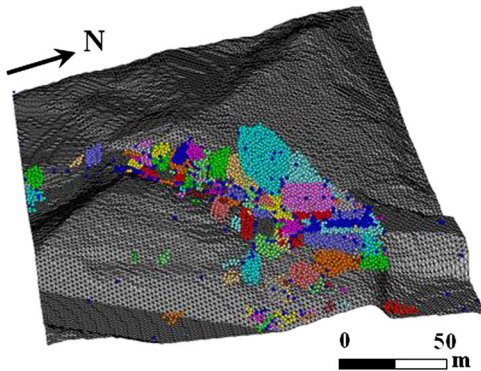
Table 4 Comparison result of modeling with different friction coefficients

| Coefficient of friction | Movement distance (m) | Deposition length (m) | Deposition wide (m) |
|-------------------------|-----------------------|-----------------------|---------------------|
| 0.3 | 0 | 0 | 0 |
| 0.2 | 0 | 0 | 0 |
| 0.1 | 0 | 0 | 0 |
| 0.05 | 0 | 0 | 0 |
| 0.04 | 185.64 | 170.21 | 144.47 |
| 0.03 | 253.23 | 182.65 | 173.51 |
| 0.02 | 263.58 | 189.25 | 176.76 |
| 0.01 | 326.45 | 201.63 | 253.97 |
| Measurement results | 259.78 | 187.78 | 174.17 |

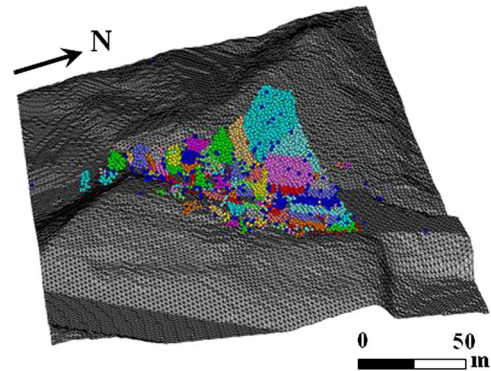
2. 0.5–2.0 s: During this period, the mean velocity of the topmost layer of the sliding mass exceeded 12.8 m/s, and the mean velocity of the bottom layers remained steady at 9.6 m/s, which was sufficient to bury the three lanes of the freeway in the Taipei-bound direction. The sliding mass had not yet crumbled, even at the time it collided with the vehicles in the first three lanes of the highway, before swiftly pushing on toward the Keelung-bound lanes. In this stage, the load pressure of the topmost layer was small relative to that of the bottom layers,

and it was not constrained by the effect of the ground anchors. A few ground anchors may still have maintained support functionality at the toe of the dip slope, or the slip surface that caused the velocity of the bottom layers was small relative to that of the topmost layer. Additionally, almost all of the ground anchors had lost support functionality at 0.5–2 s, even about 13 % of the toe of the sliding mass appeared to be in a “floating state” (this caused the contact area between the sliding mass and sliding surface to be reduced), and the static friction had

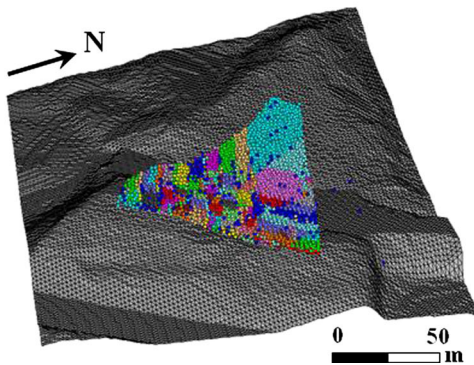
(a) Joins strength = 0.01 MPa



(b) Joins strength = 0.1 MPa



(c) Joins strength = 10 MPa



(d) Joins strength = 100 MPa

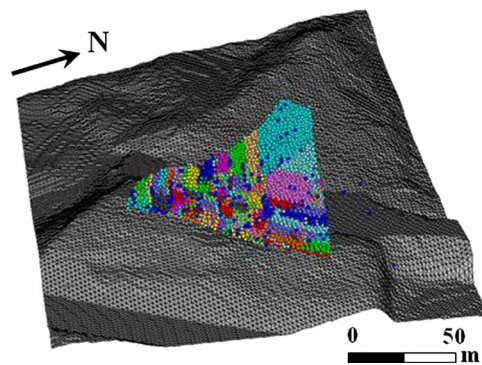


Fig. 6 Comparison result of different joints strengths

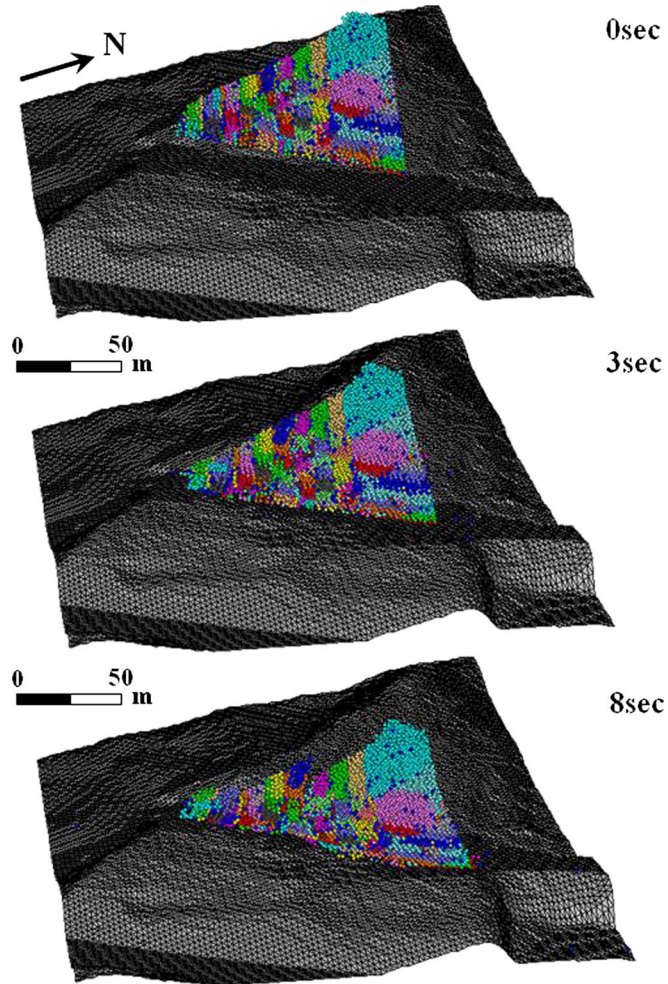


Fig. 7 Numerical modeling of the Cidu translational slide of the Formosan Freeway



(by Ministry of Transportation and Communications R.O.C, 2010)



Simulation results

Fig. 8 Compaction of the numerical simulation and aerial photos of the Cidu translational slide at the Formosan Freeway

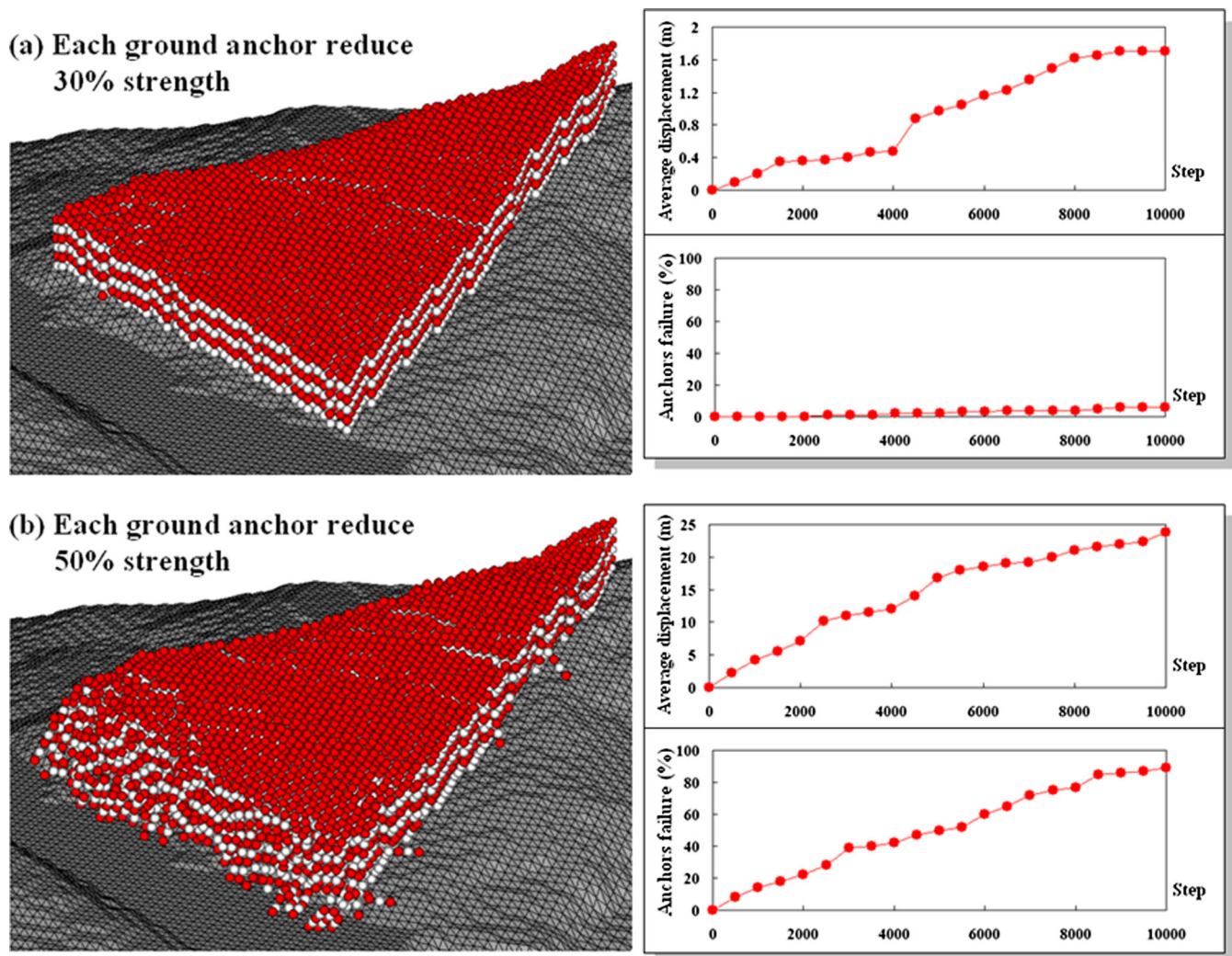


Fig. 9 Simulation results of the translational slide at the Cidu section of the Formosan Freeway with ground anchors

changed into dynamic friction of sliding mass movement, which caused the velocity of the sliding mass to increase suddenly (Fig. 10b).

3. 2.0–3.0 s: At this point, the toe of the right wing had reached the slope on the other side of the freeway and had begun to decelerating. This part of the sliding mass began to crumble along the weak plane of joint D, and some portions began to settle onto the freeway. However, the main portion of the sliding mass continued to the lanes on the far side (Fig. 10c).
4. 3.0–5.0 s: During this time, the separated portions of the right toe stopped moving, leaving them scattered between the two lanes. When the main portion of the sliding mass collided with the slope on the far side of the freeway, it continued moving up the slope. During this period, the velocity of the main sliding mass peaked (at 23.6 m/s), whereas the velocity of the right toe decreased to 2.3 m/s (Fig. 10d).
5. 5.0–7.5 s: At approximately the 5.0-s point, the main portion of the sliding mass was climbing up the slope on the far side of the freeway (Fig. 10e). Because of the slope barrier and influence of increased friction, the velocity of the sliding mass showed significant attenuation. The entire mass came to a complete stop by 7.5 s (Fig. 10f).

Evaluation of the Cidu translational slide modeling

The success of landslide modeling depends on the ability of the model to maintain consistency with observed deposits while simultaneously matching the reports of eyewitnesses and measurement data. In the current case, we sought to ensure agreement between simulation results and observations with regard to landslide volume, the position of the collapse area, and the terrain of the slip surface. Agreement between other factors was made indirectly, e.g., choosing the friction coefficient for each slip surface, the bond strength, and the contact stiffness to reproduce known patterns of deposition. Nevertheless, other consistencies that were not determined directly or indirectly were also observed:

1. Most of the proportions of materials that slid from the northwest onto the Formosan Freeway to the southeast were correct. In addition, the thickness distribution in the model closely matched the values observed throughout the deposit.
2. Approximately 20 % of the sliding mass climbed the slope on the far side of the Formosan Freeway, approximately 35 % of the sliding mass remained on the freeway, and the remainder stagnated on the slide surface. These values match the actual

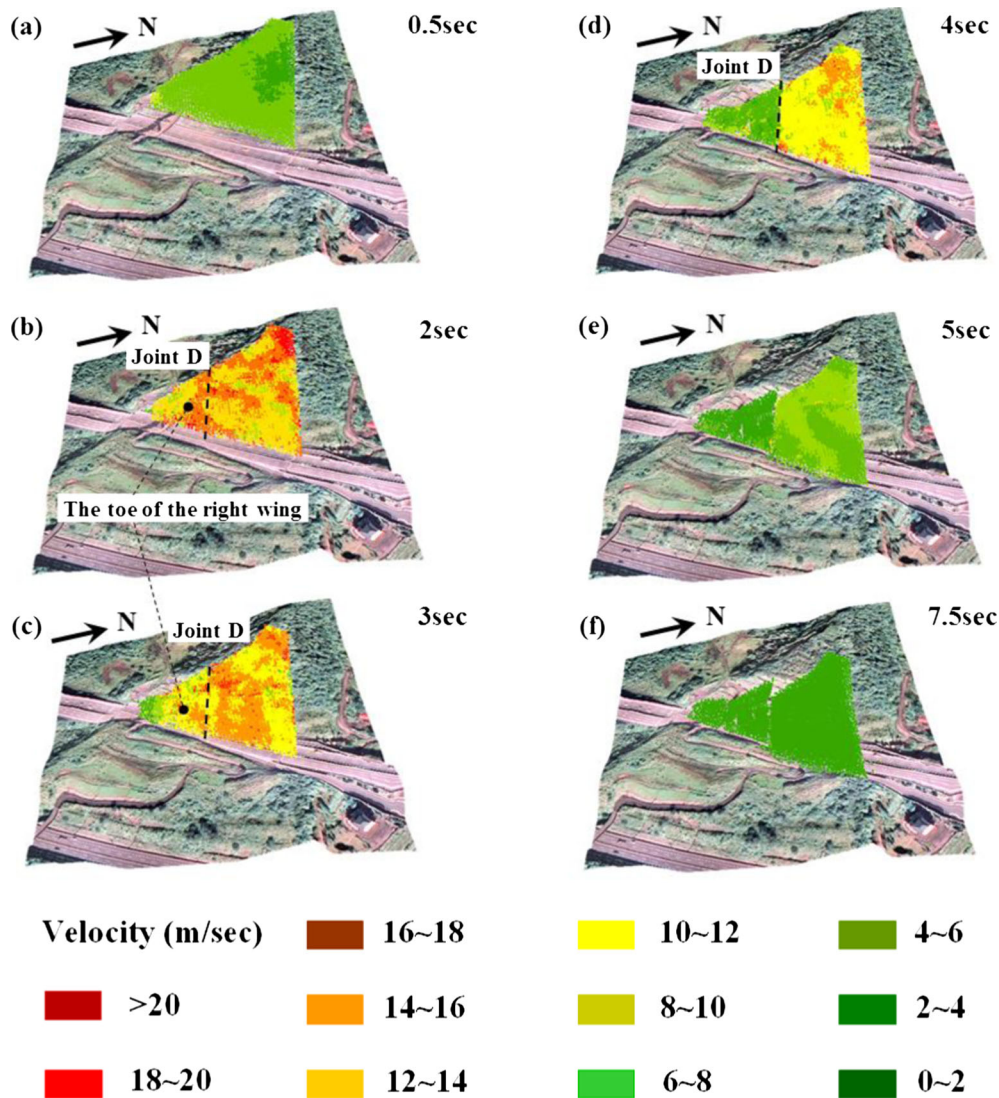


Fig. 10 Kinematic process of the translational slide at the Cidu section of the Formosan Freeway

amount of debris deposited on the freeway and opposite slope. The rather more substantial deposits on the slip surface formed a slightly fragmented deposit, providing evidence of the processes involved in the Cidu translational slide.

- Combining geomorphologic analysis and field observation is crucial to the construction of landslide models that accurately represent actual landslides (Lo et al. 2011). Wang et al. (2013) suggested a mechanism for the Cidu translational slide, which indicated that the event was caused by hollowed-out dip slope toes and infiltration of water into the surface that resulted in loss of strength in the clay-like material. This material, which is assumed to be the result of shearing during landslide movement and earlier deformation, forms a basically impermeable layer at the base of the landslide material. As a result, water pressure builds up over this layer and decreases the effective stress. This mechanism may have been the trigger initiating the Cidu translational slide. Following the initiation of movement, the clay-like material probably played an important role by forming a lubricating layer at the base of the landslide material by maintaining high pore pressure during movement (Tsou

et al. 2011). Therefore, succeeding landslide models also should follow this mechanism to reconstruct the Cidu translational slide event. The geomorphologic analysis revealed that the source area of the slip surface was covered with rock masses and joints, which we represented using ball elements with joint settings in the numerical model. Slip surfaces and irregular terrain in the study area were represented using wall elements in the construction of the terrain model. The low friction coefficient reflects a reduction in the effective friction coefficient associated with the sliding surface due to pore fluid.

Conclusion

This study used a discrete element method to simulate the kinematic processes involved in the translational slide in the Cidu section of the Formosan Freeway. We included the distribution of planes of weakness, engineering installations (the ground anchors and retaining wall), and mechanical parameters in the development of a numerical model capable of clarifying the kinematic characteristics of this translational slide with high velocities. The results indicate that within 2–4 s from initiation, the mean velocity of the sliding mass reached 10.2 m/s, such that the

freeway and three vehicles were buried almost instantaneously. In 7.5 s, the entire sliding mass came to a rest. The sliding mass formed a slightly fragmented deposit on the freeway. The results of numerical simulation are applicable of the assessment of pre-disaster scenarios and provide a valuable reference for the designation of hazardous areas associated with dip slope slides and the planning of early warning systems.

Acknowledgments

The research was mainly supported mainly by the Ministry of Science and Technology of Taiwan, Grant no. MOST 103-2625-M-270-001 and MOST 104-2625-M-270-001. The advice, comments, and help provided by the editor and reviewer have significantly strengthened the scientific soundness of this paper. Their kind assists are gratefully acknowledged.

References

- Chen MM, Wei ZY, Fei LY (2010) Analysis geology of dip slope at the Cidu section of Formosan Freeway. *Geology* 29(2):12–15 (in Chinese)
- Giani GP (1992) *Rock slope stability analysis*. Balkema, Rotterdam, p 361
- Giani GP, Migliazza M, Segalini A (2004) Experimental and theoretical studies to improve rock fall analysis and protection work design. *Rock Mech Rock Eng* 37:369–389
- Hung JJ (2010) A study on the failure and disaster prevention of dip slopes. *J Civil Hydraul Eng* 94:5–18 (in Chinese)
- Hungr O (2007) Dynamics of rapid landslides, progress in landslide science. Chapter 4, pp 47–56
- Itasca Consulting Group Inc (2002) PFC3D Particle flow code in three dimensions theory and background, Version 3.0. Minneapolis, pp 1–2
- Lin HH, Chen ZS, Chi ZC (2010) Interpretation geomorphologic of dip slope at the Cidu section of Formosan Freeway. *Geology* 29(2):20–23 (in Chinese)

- Lo CM, Lin ML, Tang CL, Hu JC (2011) A kinematic model of the Hsiaolin landslide calibrated to the morphology of the landslide deposit. *Eng Geol* 123:22–39
- Lo CM, Lee CF, Chou HT, Lin ML (2014) Landslide at Su-Hua Highway 115.9 k triggered by Typhoon Megi in Taiwan. *Landslide* 11(2):293–304
- Ministry of Transportation and Communications ROC (2010) Translational slide at the Cidu section (3K+100) of Formosan Freeway preliminary examination report. Ministr Transport Commun ROC Rep. (in Chinese)
- Potyondy DO, Cundall PA (2004) A bonded-particle model for rock. *Int J Rock Mech Min Sci* 41:1239–1364
- Steven NW, Simon D (2006) Particulate kinematic simulations of debris avalanches: interpretation of deposits and landslide seismic signals of Mount Saint Helens, 1980 May 18. *Int J Geoph* 167:991–1004
- Taiwan Geotechnical Society (2011) Summary report of investigation of reasons for Taiwan freeway No. 3 (Formosan Freeway Cidu section) 3 k+300 m landslide. Rep. prepared by Taiwan Geotechnical Society for Ministry of Transportation and Communication, Taiwan: 16–79 [in Chinese]
- Tsou CY, Feng ZY, Chigira M (2011) Catastrophic landslide induced by Typhoon Morakot, Shialin, Taiwan. *Geomorphology* 127:166–178
- Wang L, Hwang JH, Luo Z, Juang CH, Xiao J (2013) Probabilistic back analysis of slope failure—a case study in Taiwan, 1980 May 18. *Comput Geotech* 51:12–23

C.-M. Lo (✉)

Department of Civil Engineering,
Chienkuo Technology University,
Changhua, Taiwan, Republic of China
e-mail: ppb428@yahoo.com.tw

H.-H. Li

Department of Environmental Information and Engineering,
National Defense University,
Taoyuan, Taiwan, Republic of China

C.-C. Ke

Geotechnical Engineering Research Center,
Sinotech Engineering Consultants, Inc.,
Taipei, Taiwan, Republic of China